

Washington University School of Medicine Digital Commons@Becker

Open Access Publications

2015

Strengths and weaknesses of a planar whole-body method of ^{153}Sm dosimetry for patients with metastatic osteosarcoma and comparison with three-dimensional dosimetry

Donika Plyku

Johns Hopkins University

David M. Loeb

Johns Hopkins University

Andrew Prideaux

Johns Hopkins University

Sébastien Baechler

University of Lausanne

Richard L. Wahl

Washington University School of Medicine in St. Louis

See next page for additional authors

Follow this and additional works at: http://digitalcommons.wustl.edu/open_access_pubs

Recommended Citation

Plyku, Donika; Loeb, David M.; Prideaux, Andrew; Baechler, Sébastien; Wahl, Richard L.; Sgouros, George; and Hobbs, Robert F., "Strengths and weaknesses of a planar whole-body method of ^{153}Sm dosimetry for patients with metastatic osteosarcoma and comparison with three-dimensional dosimetry." *Cancer Biotherapy and Radiopharmaceuticals*.30,9. 369-379. (2015).
http://digitalcommons.wustl.edu/open_access_pubs/4407

This Open Access Publication is brought to you for free and open access by Digital Commons@Becker. It has been accepted for inclusion in Open Access Publications by an authorized administrator of Digital Commons@Becker. For more information, please contact engeszer@wustl.edu.

Authors

Donika Plyku, David M. Loeb, Andrew Prideaux, Sébastien Baechler, Richard L. Wahl, George Sgouros, and Robert F. Hobbs

Strengths and Weaknesses of a Planar Whole-Body Method of ^{153}Sm Dosimetry for Patients with Metastatic Osteosarcoma and Comparison with Three-Dimensional Dosimetry

Donika Plyku,¹ David M. Loeb,¹ Andrew R. Prideaux,¹ Sébastien Baechler,² Richard L. Wahl,^{1,*} George Sgouros,¹ and Robert F. Hobbs¹

Abstract

Purpose: Dosimetric accuracy depends directly upon the accuracy of the activity measurements in tumors and organs. The authors present the methods and results of a retrospective tumor dosimetry analysis in 14 patients with a total of 28 tumors treated with high activities of ^{153}Sm -ethylenediaminetetramethylenephosphonate (^{153}Sm -EDTMP) for therapy of metastatic osteosarcoma using planar images and compare the results with three-dimensional dosimetry.

Materials and Methods: Analysis of phantom data provided a complete set of parameters for dosimetric calculations, including buildup factor, attenuation coefficient, and camera dead-time compensation. The latter was obtained using a previously developed methodology that accounts for the relative motion of the camera and patient during whole-body (WB) imaging. Tumor activity values calculated from the anterior and posterior views of WB planar images of patients treated with ^{153}Sm -EDTMP for pediatric osteosarcoma were compared with the geometric mean value. The mean activities were integrated over time and tumor-absorbed doses were calculated using the software package OLINDA/EXM.

Results: The authors found that it was necessary to employ the dead-time correction algorithm to prevent measured tumor activity half-lives from often exceeding the physical decay half-life of ^{153}Sm . Measured half-lives so long are unquestionably in error. Tumor-absorbed doses varied between 0.0022 and 0.27 cGy/MBq with an average of 0.065 cGy/MBq; however, a comparison with absorbed dose values derived from a three-dimensional analysis for the same tumors showed no correlation; moreover, the ratio of three-dimensional absorbed dose value to planar absorbed dose value was 2.19. From the anterior and posterior activity comparisons, the order of clinical uncertainty for activity and dose calculations from WB planar images, with the present methodology, is hypothesized to be about 70%.

Conclusion: The dosimetric results from clinical patient data indicate that absolute planar dosimetry is unreliable and dosimetry using three-dimensional imaging is preferable, particularly for tumors, except perhaps for the most sophisticated planar methods. The relative activity and patient kinetics derived from planar imaging show a greater level of reliability than the dosimetry.

Key words: dosimetry, imaging, radionuclide therapy, radiopharmaceuticals, osteosarcoma

Introduction

The purpose of dosimetry is to deduce dose–response relationships for tumors and normal organs, as well as to bring patient-based treatment planning to the clinic based on

these relationships. The accuracy and therefore the ability of dosimetry to perform accordingly depend highly upon the accuracy of the activity measurements in the tumors and organs. Planar image quantification, which has long been the principal means of activity quantification used as an input

¹Department of Radiation Oncology, Johns Hopkins University School of Medicine, Baltimore, Maryland.

²University Institute of Radiation Physics, University of Lausanne, Lausanne, Switzerland.

*Currently at the Malinckrodt Institute of Radiology, Washington University, St. Louis, Missouri.

Address correspondence to: Robert F. Hobbs; Department of Radiation Oncology, Johns Hopkins University School of Medicine; CRB II 4M.60, 1550 Orleans Street, Baltimore, MD 21231
E-mail: rhobbs3@jhmi.edu

into the calculation of absorbed dose,¹ requires an extensive array of methodological adjustments for scatter correction,^{2–5} attenuation,^{6–8} septal penetration, and, most recently, dead-time correction for whole-body (WB) images involving the relative motion between the camera and imaged object,⁹ with an end result that is still controversial. In particular, He et al.^{10,11} showed, in the context of phantom studies, an absolute uncertainty of 30% in planar quantification compared with 5% using single-photon emission computed tomography (SPECT) images; the relative quantification, that is, determination of kinetic parameters, is considered to be more reliable^{4,12} as the errors from scatter, septal penetration, and attenuation generally cancel out from one time point to the next for the same imaged object. As yet, no such comparison has been extended to clinical data where certain methodological components present a much greater challenge and the potential for increased uncertainty. In particular, the issue of background subtraction becomes more problematic as the superposition of different anatomical features with varying uptakes and depths creates a nonuniform landscape from which it is difficult to extract a reasonable background rate with any accuracy, certainly not with a strictly systematic methodology, and where *ad hoc* adjustments are often required to determine background rates.

The use of ¹⁵³Sm-ethylenediaminetetramethylenephosphonate (¹⁵³Sm-EDTMP) for palliative treatment of bone metastases from a variety of carcinomas is well established,^{13–16} and its therapeutic value for patients with osteosarcoma is being investigated.^{17–20} Sm-153-EDTMP, or Quadramet™, is a bone-seeking calcium mimetic containing the ¹⁵³Sm radionuclide, which decays by β^- emission, with a half-life of 46.5 hours and a maximum β^- energy of 808 keV. Sm-153 also emits photons, including a 103 keV photon with 28.3% frequency, which is used for quantitative imaging. This radiopharmaceutical targets new pockets of calcification such as are seen in bony metastases from epithelial tumors and in osteosarcoma. The calcification of new osteosarcoma lesions is in general very rapid so that even recently established tumors can most often be imaged and treated. Any other region of the body that has new calcification will also show uptake of ¹⁵³Sm-EDTMP, including, but not limited to, bone that is stressed, epiphyseal growth plates, and bone that has had recent lesions.²¹ This bone uptake constitutes the large part of the background in the images. Typically, an order of magnitude more of uptake in bone tissue than in soft tissue can be seen, with another order of magnitude (or more) of uptake present in the tumor sites.

Although biodistribution and dosimetry studies of ¹⁵³Sm-EDTMP have been conducted on animals,^{22–24} the existing human data are almost exclusively in patients with bone metastases of epithelial cancers^{25–31} or for bone marrow transplant³² or toxicity studies³³ where the focus is not on dosimetry, although with a few notable exceptions.^{17,34}

In this study, the authors present the methods and results of a retrospective planar imaging-based tumor dosimetry analysis in 14 metastatic osteosarcoma patients treated with ¹⁵³Sm-EDTMP, which complements previously published clinical results.^{19,20,34,35} Because of the high activities involved, camera saturation effects occur and affect quantitative as well as qualitative analysis. Incorrect quantification could lead to false half-life estimations, which would lead to erroneous conclusions concerning the biological dynamics

of the activity distribution in the body. To account for these effects, the authors used a previously described method for saturation compensation in cases of relative motion between the detector and patient.⁹

The main purpose of this study is to determine the reliability of planar-based dosimetry in clinical data by comparing the relative differences of the anterior and posterior dosimetric values from a set of tumor data for an empiric quantification of the uncertainty in two-dimensional dosimetry. A comparison between two-dimensional and three-dimensional dosimetric results (previously published³⁴) for a set of same tumors and a comparison of the differences in the relative uncertainties estimated in phantoms^{11,36} are also undertaken with this objective in mind. In addition, the authors will also compare dosimetric values between the same tumors at different initial dose values and determine the strength of the correlation between the uptakes at two different administered activities.

Materials and Methods

Patients and ¹⁵³Sm-EDTMP therapy

A phase I dose-finding study of patients with high-grade osteoblastic osteosarcoma was conducted to determine the maximum tolerated injected activity of ¹⁵³Sm-EDTMP with hematopoietic recovery within 6 weeks. Subsequently, a phase II study was performed to assess the safety and response of high-risk osteosarcoma to a high injected activity of ¹⁵³Sm-EDTMP, and 11 of 14 patients who participated in the phase I study were determined to be eligible to receive a second high injected activity (tandem dose) of ¹⁵³Sm-EDTMP. Seven of these patients were imaged for dosimetric purposes. Loeb et al.^{19,20} have described the clinical trial details and the treatment plan. Briefly, patients with a positive ^{99m}Tc-methylene diphosphonate bone scan finding were included in the study and autologous hematopoietic stem cells were collected before the first treatment with ¹⁵³Sm-EDTMP (low injected activity), which ranged from 37 to 51.8 MBq/kg (1.0–1.4 mCi/kg). Patients were followed up until hematologic recovery and evaluated for disease response. Approximately 6 weeks after the first treatment, a second treatment (high injected activity) with 222 MBq/kg (6 mCi/kg) of ¹⁵³Sm-EDTMP was administered. Patients received autologous stem cell infusion 14 days after high injected activity ¹⁵³Sm-EDTMP therapy. The study was approved by the institutional review board of Johns Hopkins University and informed consent was provided by all patients or their legal guardian. The data were collected from 14 metastatic osteosarcoma patients (ages 11–30 years, mean 18, median 18). The patients presented with a total of 28 tumors (mass 5 g–4 kg, mean 326 g, median 30 g). More detailed patient information is given in Table 1.

Quadramet (¹⁵³Sm-EDTMP) targets new pockets of calcification and therefore does not, in principle, target the earliest form of the disease, which is a soft tissue disease which calcifies. However, the calcification is in general very rapid so that even recently established tumors can most often be imaged and treated. ¹⁵³Sm-EDTMP can be used to target relatively new disease, which has already accrued mass and calcium deposit, but not disease at the cellular level in the blood stream, for example. Any other region of the body that has new calcification will also show uptake of ¹⁵³Sm, including, but not limited to, bone that is stressed or that has had recent lesions. This bone uptake constitutes the

TABLE 1. CLINICAL PATIENT AND TUMOR INFORMATION

Patient	Sex	Age	Mass (kg)	AA (GBq)	Tumor	Tumor location	Tumor mass (g)
1	F	18	61.0	3.16	1	L2 vertebra	34.0
2	M	11	64.5	3.57	2	Shoulder	22.2
					3	Hip	25.7
3	M	17	67.0	3.50	4	Pelvic node	5.72
4	F	30	52.0	2.37/11.5	5	Abdomen	210/379
					6	Sternum	10.9/20.6
					7	Chest wall	n.a./18.3
					8	Chest wall	n.a./21.6
5	M	20	95.0	4.20	9	Shoulder	47.6
6	M	15	70.0	3.26/16.7	10	L1 vertebra	14.9
					11	Femur	20.7
					12	Femur	5.05
7	M	15	62.0	2.72/15.4	13	Mandible	21.2
8	F	14	46.0	1.78/9.43	14	Paraspinal	3.52/50.0
9	F	19	70.0	2.84/16.6	15	Skull	26.4
					16	Left clavicle	n.a./25.1
					17	Posterior rib	n.a./15.0
					18	Mediastinum	n.a./23.6
					19	Back	n.a./18.0
					20	Umbilicus	n.a./41.4
10	M	21	53.0	2.13	21	Abdomen	4130
					22	Abdomen	118
11	M	12	52.0	2.39	23	Knee	633
12	M	21	76.5	3.57/17.0	24	Spine	43.2/266
					25	Hip	25.1/36.3
13	M	25	100.5	3.73	26	Hip	482
14	F	25	84.5	3.93/17.8	27	Hip	65.3/1050
					28	Chest	n.a./17.0

When data from both low and high activity regimens are available, both are given, separated by a slash. Tumors that were not present for the low activity regimen are designated by “n.a.”
AA, administered activity.

large part of the background in the images. Typically, for the administered activity range in this study, an order of magnitude more of uptake in bone tissue than in soft tissue can be seen, with another order of magnitude (or more) of uptake present in the tumor sites.

Imaging

Patients were imaged on a GE Infinia Hawkeye gamma camera using a low-energy high-resolution collimator for the low activity regimen and a medium-energy general-purpose collimator for the high activity regimen, using an energy window set at 103 ± 10.3 keV; a sample image is shown in Figure 1. WB scans (Fig. 1) were collected at a sweep rate of 10 cm/minute. Since scatter windows were not set at study acquisition time, scatter correction was performed using a buildup factor correction term.^{3,37} Calibration, scatter, attenuation, and count dead-time corrections were implemented as outlined below and in a previous study.⁹

In addition, SPECT/CT imaging was done on a subset of the patient population. This allowed for three-dimensional tumor dosimetry using 3D-RD, a personalized dosimetry software package.^{38,39} The results of that analysis have been published³⁴ and were available for comparison with the planar dosimetry.

Dead-time correction

The counts of all the pixels in a same row are affected by saturation in the same proportion. As illustrated in Figure 1a

and b, the measured count values were summed for each pixel row (y values) and the corrections were made on a row-by-row basis by applying a previously published methodology developed for this specific purpose.⁹ The implementation of this methodology requires a translation of the counts measured spatially to a time-ordered measure of counts, that is, the counts measured as a function of time. This is necessary as the camera dead time is a function of the activity seen by the whole camera and thus the saturation for a specific y-row varies as a function of time as the camera sweeps over all positions, which include y. Thus, the activity quantification does not depend on a single conversion, but is a function of the activity (or count rate) itself and is incorporated into the dead-time effect calculations. Figure 1b shows the number of counts measured as a function of y-position, while Figure 2 shows the specifics of the modifications made to the measured counts. Figure 2a shows the number of counts measured as a function of time, that is, related to the activity seen by the camera at time t. The counts as a function of time (or camera position relative to the patient) are corrected by the factor shown in Figure 2b using a multidimensional adaptation of Newton’s method, and the correction factor is then translated to the spatial distribution of counts (y-row values) (Fig. 2c).

WB half-lives

A check on the correction algorithm for count rate saturation was made by examining the WB clearance half-lives

FIG. 1. Count image of a patient (left panel). They y-axes are the same for both images. In the right panel, the x-axis shows the sum of the counts measured across the y-row of pixels in the left panel.

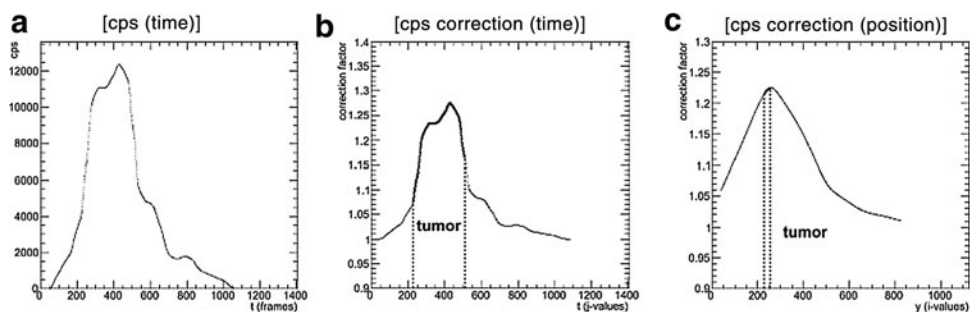
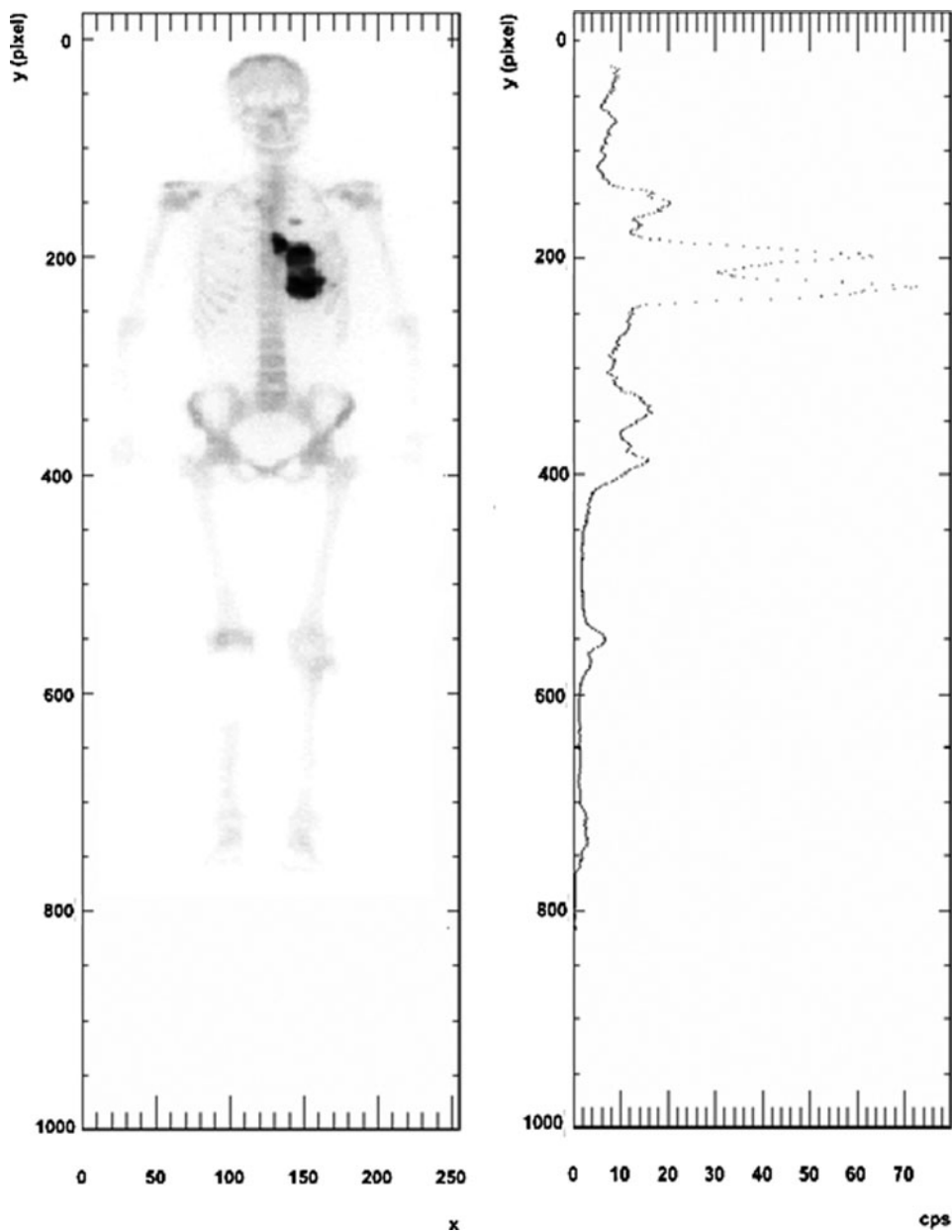


FIG. 2. Camera dead-time algorithm applied to the patient data shown in Figure 1. (a) Shows the counts seen by the camera as a function of time as the camera passes over the patient starting from the head. (b) Shows the correction values calculated using the algorithm as a function of time. (c) Shows the correction translated back into y-row values. Note that the time that the camera passes over the tumor is longer than the time to travel the distance taken up by the tumor, therefore the tumor extent is greater in the time frame (a, b) than in the physical space (c).

TABLE 2. THE NONSATURATION-CORRECTED EFFECTIVE WB HALF-LIVES (MEAS. WB HL) AND SATURATION-CORRECTED EFFECTIVE WB HALF-LIVES (CORR. WB HL)

Patient	Meas. WB HL (hours)	Corr. WB HL (hours)
1	41.7	39
2	59.9	53.8
3	47.8	44.9
4	48.3/55.0	44.6/45.8
5	45.9	41.2
6	50.1/57.0	47.5/49.7
7	37.4/38.8	35.0/35.4
8	37.6/34.4	35.7/31.4
9	36.3/43.3	34.0/41.5
10	49.5	45.4
11	47.3	13.7
12	47.2/48.1	45.0/45.5
13	52	49.5
14	35.7/42.6	33.2/37.0
M	45.5/45.6	42.3/40.9
SD	6.7/7.7	6.0/6.1

Low and high activity data are separated by a slash.
HL, half-life; M, mean; SD, standard deviation; WB, whole-body.

obtained for each patient before and after correction for count rate saturation. The WB effective half-time values are given in Table 2; for comparative purposes, the authors also present the noncorrected values. The half-life was obtained by fitting a monoexponential fit to the WB counts at the different time points. The WB counts were taken as the geometric mean of the posterior and anterior counts.

Tumor dosimetry

The tumor masses and depths from the anterior and posterior surfaces were determined from CT images acquired a few days before WB planar imaging. The tumor time-activity curves were obtained by drawing tumor regions of interest (ROIs) defined by a threshold of the maximum count value of each individual tumor on anterior and posterior planar images, respectively, which had been previously corrected for count saturation. A core feature of the MIRD anteroposterior methodology of activity determination is the background subtraction. Since the activity measured at the surface of the ROI is the sum of the contribution from the tumor as well as the background activity present in the patient both in front of and behind the tumor, the background activity must be estimated and its contribution to the ROI activity subtracted. For this, a region must be determined where the activity is assumed to be homogeneously distributed as a function of patient depth and is consistent with the background activity present at the level of the ROI. In this methodology, the tumor region is grown from a seed visually placed in a region of high count rate and using a threshold determined experimentally to give an area corresponding visually to the activity from the tumor in question. The background region is determined graphically by symmetry of the tumor with respect to the vertical axis, but with a condition that there be no overlap and with a spacing of a minimum of five voxels between the tumor and background. Figure 3 shows an example of a tumor region and a background region, determined using this procedure.



FIG. 3. Count image of the tumor (right image) and background (left image) shown in Figure 1. The background region is determined by symmetry of the tumor with respect to the vertical axis, but with a condition that there be no overlap and with a spacing of a minimum of five voxels between the tumor and background.

The counts in the tumor ROIs were scatter and attenuation corrected using a buildup factor method,³ as implemented in a previous publication.⁹ The tumor activity was then determined by applying the sensitivity and dead-time conversion and taking the geometric mean of the anteriorly and posteriorly determined activities. The time-integrated activity for each tumor was obtained by analytically integrating a simple exponential function to the time-activity data for each tumor. The time-integrated activity coefficient (residence time) was then entered into the OLINDA/EXM⁴⁰ tumor dose sphere module and the absorbed dose for each tumor was obtained. Note that most patients presented with two time points of imaging, therefore no quantitative evaluation of the goodness of fit was available.

A few patients also were imaged using the SPECT/CT camera and the 3D dosimetry was performed using the 3D-RD personalized dosimetry package.^{38,39} The results from this work have been published³⁴ and served as a comparison for the planar dosimetry results.

Note that the size and location of the tumors are quite diverse (Table 1). Tumors for which there was no CT imaging available were not taken into consideration. Neither did the authors include tumor sites near prosthetics, which create too much scatter in the CT and falsify the density values, as well as make the tumor contours difficult to detect.

The average depths of the tumor from the anterior and posterior body surfaces are also measured using these CT images. These values are then used to calculate photon attenuation through the body tissue, using the buildup factor method.³

Uncertainty analysis

A first-order estimate of the uncertainty in tumor activity calculations was obtained by comparing the estimated anterior and posterior activities to the value obtained by the conjugate view method.^{37,41} In principle, the activity in a tumor can be measured from a single 2D view by measuring the counts in an ROI drawn around the tumor:

$$A_0 = s \cdot C_{A/P} \cdot e^{\mu d_{A/P}} \tag{1}$$

where $C_{A/P}$ are the counts measured on either the anterior (A) or posterior (P) view, respectively, in the ROI drawn

around the tumor; s is the sensitivity, which converts counts to activity; and the exponential is the factor that accounts for attenuation, with μ as the attenuation coefficient and $d_{A/P}$ as the depth of the tumor seen from the anterior (A) or posterior (P) side, respectively. The sensitivity is not applied as a single value, but is incorporated in the dead-time saturation curve, which gives the count rate as a function of activity. This formulation is valid in cases where the anterior–posterior thickness of the tumor is much smaller than the overall anterior–posterior thickness of the patient; otherwise, an integration of the exponential over the thickness of the tumor is necessary. Equation (1) yields only an approximate estimate of the tumor activity since it is valid only when there is no activity outside of the tumor contributing to the measured counts, which is rarely the case. In general, background subtraction is necessary. This single formula has the disadvantage of requiring some three-dimensional information, namely the depth of the tumor, usually obtained with a CT scan; however, since it is valid for both views, the product of the two views gives the following:

$$A_0^2 = s^2 C_A C_P \cdot e^{\mu(d_A + d_P)} \quad (2)$$

Since $d_A + d_P$ is the thickness of the patient (D), which may be obtained without 3D imaging, the basic equation for the conjugate view method when the tumor is small and tumor self-attenuation may be neglected is as follows:

$$A_0 = s \sqrt{C_A C_P} \cdot e^{\mu D} \quad (3)$$

This approach is adopted even when three-dimensional information is available and utilized in more sophisticated calculations, such as including tumor self-attenuation and background subtraction, which may be generalized as follows:

$$A_0 = \sqrt{A_A A_P} \quad (4)$$

where A_A and A_P are the activities calculated from the counts measured in the ROI from the anterior (A) and posterior (P) images, respectively. In principle, if all the appropriate corrections are made, both are equal to A_0 . By calculating the difference between A_0 calculated from the posterior and anterior views, an indication of the uncertainty in the values of the activity may be obtained as follows:

$$\frac{A_0 - A_{A/P}}{A_0} \quad (5)$$

The relative difference between anterior and posterior activity is given by the following:

$$2 \frac{A_A - A_P}{A_A + A_P} \quad (6)$$

Low activity–high activity comparison

While the dosimetry based on planar imaging quantification remains questionable, planar imaging is generally considered reliable for relative quantification. When available, a comparison was made between the calculated absorbed doses

delivered to the same tumor for both regimens, the low activity (1.0–1.4 mCi/kg) and high activity (6.0 mCi/kg), to determine if a five-fold increase in activity results in a comparable increase in uptake and tumor-absorbed dose.

Results

WB half-lives

A check on the correction for count rate saturation was made by examining the WB clearance half-times obtained for each patient before and after correction for count rate saturation. The WB effective half-time values are given in Table 2. The mean \pm standard deviation for the uncorrected measured effective WB half-time was 45 ± 6 hours. The dead-time correction model gave 42 ± 6 hours; these should be compared with the physical decay half-life for ^{153}Sm , which is 46.5 hours. More specifically, 11 half-lives were measured as being nonphysical (longer than 46.5 hours) before dead-time correction, while 4 half-lives were still nonphysical after dead-time correction.

Tumor radiation-absorbed dose

The absorbed dose values obtained using the OLINDA/EXM homogeneous spherical model are shown in Table 3, along with the previously published results from the three-dimensional analysis.³⁴

A relationship between the time-integrated activity coefficient, τ , and the tumor mass, m , was examined. Inspired by the mass uptake dependency proposed by Williams et al.,⁴² in theory applicable to high-molecular-weight antibodies, τ was plotted against m using both the planar (Fig. 4a) and three-dimensional uptake values (Fig. 4b). Fits of the form of the following equation:

$$\tau = am^b \quad (7)$$

where a and b are the parameters were made to both sets of data. The planar imaging-derived data gave a value of $a = 0.00429$ h/g and $b = 0.91$, with a correlation coefficient of $R^2 = 0.72$. For the three-dimensional data from 3D-RD, the values were $a = 0.00340$ h/g, $b = 1.08$, and $R^2 = 0.74$.

Anteroposterior activity comparison

An assessment of the uncertainty in activity quantification and the absorbed dose estimates was obtained by comparing the anterior and posterior tumor activity calculations. The standard deviation, or σ value, of the percentage difference using Equation (2) is 35.6%. A commonly used value for uncertainty is 2σ , which corresponds to a 95% confidence interval; thus, the uncertainty on the tumor-absorbed dose values as ascertained empirically is on the order of 71.2%. Using Formula (3), the standard deviation is 72.5%. Both sets of results were obtained using 99 of the 112 tumor images (multiple time points per tumor). The remaining 13 values could not be calculated since 1 of the 2 values (anterior or posterior) gave completely nonsensical activity values (could not be distinguished from the background).

3D-RD comparison

The absorbed dose values that were calculated by both the planar and the three-dimensional methodologies were

TABLE 3. DOSIMETRY RESULTS FOR 28 TUMORS FROM 14 PATIENTS

Tumor No.	TIA_{low} (GBq-h)	HL_{low} (hours)	AD_{low} (Gy)	AD_{low} (3D) (Gy)	TIA_{high} (GBq-h)	HL_{high} (hours)	AD_{high} (Gy)	AD_{high} (3D) (Gy)
1	0.417	51.9	1.91	—	—	—	—	—
2	0.630	55.2	4.40	—	—	—	—	—
3	0.566	54.9	3.42	—	—	—	—	—
4	0.0392	61.2	1.04	—	—	—	—	—
5	8.32	45.8	6.34	14.6	25.2	64.4	10.7	59.3
6	0.0674	74.2	0.95	1.48	0.861	64.4	6.47	21.9
7	—	—	—	—	0.746	41.7	6.30	28.4
8	—	—	—	—	0.0982	30.2	0.70	28.6
9	0.925	58.2	3.05	—	—	—	—	—
10	0.167	105.2	1.72	—	0.620	45.2	6.40	—
11	0.616	39.8	4.62	—	3.89	47.8	29.1	—
12	0.0371	44.3	1.12	—	0.304	51.8	9.14	—
13	0.244	58.0	1.78	—	1.48	48.4	10.8	—
14	0.0509	32.4	2.18	—	1.68	49.4	5.28	—
15	0.303	—	1.79	—	2.84	74.4	16.7	—
16	—	—	—	—	0.514	43.6	3.18	2.93
17	—	—	—	—	0.333	42.6	3.42	3.09
18	—	—	—	—	0.218	45.8	1.44	3.13
19	—	—	—	—	0.779	50.5	6.69	5.45
20	—	—	—	—	0.536	47.1	2.03	3.33
21	13.4	46.8	0.54	—	—	—	—	—
22	0.846	50.0	1.14	—	—	—	—	—
23	5.59	41.4	1.44	2.06	—	—	—	—
24	0.883	49.0	3.20	5.45	23.1	49.2	14.0	21.6
25	0.323	42.1	2.00	3.18	1.87	48.8	8.03	23.8
26	4.07	31.0	1.37	2.85	—	—	—	—
27	0.373	37.5	0.90	1.80	2.49	—	0.39	0.79
28	—	—	—	—	0.698	—	6.33	13.1
M	1.89	51.52	2.25	4.49	3.75	49.72	7.82	16.86
SD	3.47	16.71	1.50	4.65	7.50	10.09	6.96	17.35

The (low) index indicates the low activity results, the (high) index indicates high activity results. AD, absorbed dose; TIA, time-integrated activity.

compared (Fig. 4c). However, only a weak correlation was apparent ($R^2=0.44$ for a linear correlation). Moreover, the average ratio of 3D absorbed dose value to 2D absorbed dose was 2.13 ± 1.22 , excluding tumor No. 8, which had a ratio of 40.9.

Low activity–high activity comparison

Ten tumors in 7 patients were imaged for both the low-dose (~1 mCi/kg) and high-dose (~6 mCi/kg) regimens. A comparison was made between the absorbed dose values. The average ratio was 5.29 ± 2.38 , which is on the order of the ratio of activities. However, the dispersion of values is relatively large, and by plotting the low activity absorbed dose (AD)

values versus the high-dose AD values (Fig. 5), a linear best fit gives a slope, m , of only 1.98 with a y-intercept of $b=6.57$ with a fit value of $R^2=0.71$ (blue line). Fitting the average value gives a correlation of only $R^2=0.44$ (red line). However, by omitting the outlier tumor No. 5, with a low activity/high activity ratio of 1.69 (and with a ratio of 4.06 measured with 3D-RD), a better correlation exists, $R^2=0.87$.

Discussion

A retrospective planar imaging-based dosimetry analysis was performed on osteosarcoma patients administered ¹⁵³Sm-EDTMP with therapeutic intent. As suggested by the uncorrected WB clearance half-times (Table 2), being

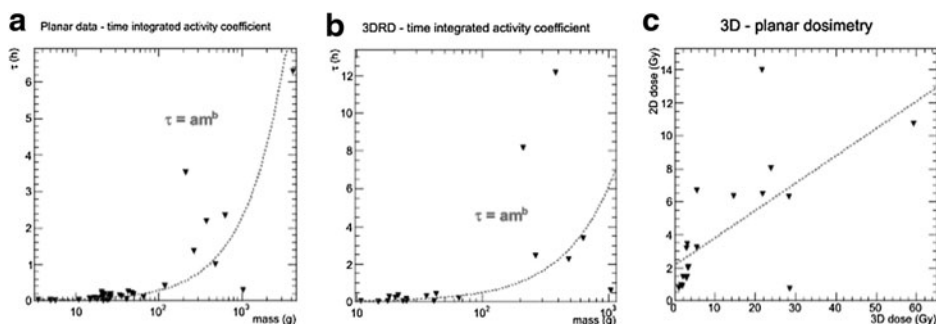


FIG. 4. (a) Time-integrated activity coefficient as a function of mass in a semilog plot using results from the two-dimensional analysis. The dotted line shows the power function fit. (b) Shows a similar fit using the data from the 3D-RD analysis. (c) Shows the planar absorbed dose values as a function of the 3D-RD absorbed dose values.

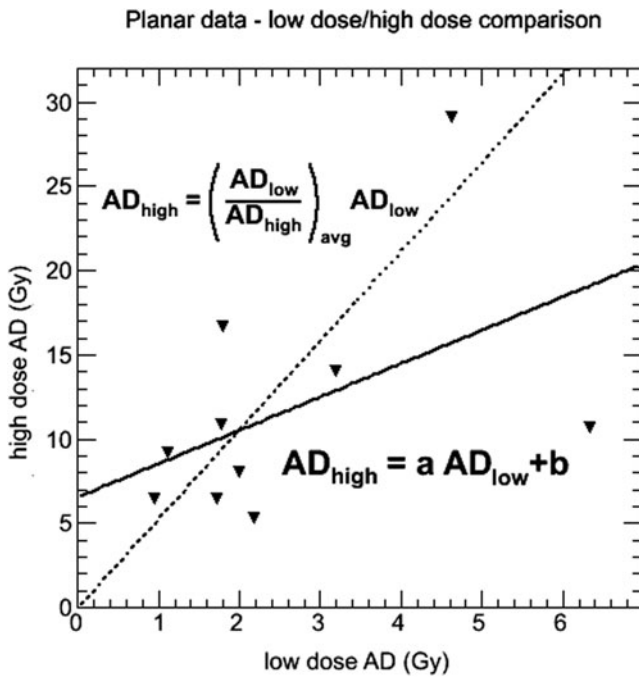


FIG. 5. Low activity results plotted versus the high activity results from the planar dosimetry. The *solid line* shows the fit result, while the *dotted line* represents the average ratio relationship.

longer than the physical half-life of ^{153}Sm , a correction for count saturation was required. The count dead-time correction yielded WB half-lives consistent with the physical decay half-life of the radionuclide.

The correction method used to account for dead time, although quite developed, is still a simplification of a complex phenomenon; in particular, dead time contribution may come from photons reaching the collimator from outside the field of view. Similarly, the assumption that counts of all the pixels in a same row are affected by saturation in the same proportion is a simplification as the count rate degradation of image quality is not uniform across the entire field of view or over the same row. Therefore, although the data point to a reasonable first-order dead-time correction, there is still ample room for improvement of the methodology.

From an uncertainty standpoint, the comparison of the corrected tumor activity for each view with a conjugate view activity measure shows that the corrections applied yielded an uncertainty of $\sim 71\%$ for the calculated tumor dose estimates. This is higher even than the values (30%) found in phantom studies,¹¹ although not surprising since the additional complications of overlapping regions and nonuniform background activity make quantification in patients more complex and thus less accurate. Note that the 71% value is an estimate from relative values used to calculate an activity which is unknown, as opposed to the phantom studies where the uncertainty is measured relative to a known truth. Additionally, this value is minimized since in 13 of 112 instances values could not be calculated given that either the anterior or posterior activity value could not be determined. The comparison with the three-dimensional results suggests an equally large

discrepancy: on average, the two-dimensional dosimetry gave absorbed dose values more than two times lower than the 3D-RD values.

The foregoing estimate of uncertainty should be considered when interpreting the results of any analysis using activity quantification or dosimetry based on planar imaging. For example, the reliability of the power function fit of the tumor uptake-versus-mass data (Fig. 4a), despite a reasonably high correlation coefficient, is questionable. On the other hand, a similar fit can be seen with the 3D-RD-derived absorbed dose values, although the values of the fitted parameters are different, which is not surprising given the lack of correlation between the two-dimensional and three-dimensional results (Fig. 4c). It must be noted that a strong correlation was previously observed³⁴ between the absorbed dose from two distinct three-dimensional methodologies, 3D-RD and OLINDA/EXM, using activity acquired from SPECT scans, with the differences (on the order of 5%–10%) being attributed to the lack of external contribution in the OLINDA/EXM simple sphere model. Thus, it appears that the large discrepancies are indeed attributable to the planar activity quantification and methodology, although uncertainties are certainly present in the 3D-RD analysis. In general, it must be stated that a lack of uncertainty or error estimate attached to absorbed dose values regardless of methodology contributes to a general skepticism of dosimetry, where it becomes difficult to appreciate the value of the results, and efforts need to be made to establish methodologies, which will enable a systematic presentation of dosimetric results with error bars. While efforts are indeed underway in this direction, no general methodology has yet been established.

The WB half-life results confirm the value of the camera saturation algorithm as well as confirm that the relative dosimetry is indeed more reliable than absolute quantification for planar dosimetry, as indicated in the literature.^{4,12} The average measured tumor half-times are on the order of the physical decay half-life of 46.5 hours, confirming previously published results,²⁸ although with a much greater variability than with the WB results. As a first approximation, the ^{153}Sm -EDTMP binds to the tumor site such that there is relatively little biological clearance, unlike high-molecular-weight antibody agents, which have a more prolonged uptake time.⁴³ However, the tumor half-life results suggest some amount of tumor uptake beyond the first time point (4 hours), although the nature of the tumor dosimetry methodology, in particular the background subtraction, suggests caution in this assessment.

Given the more reliable nature of the relative dosimetry, that is, the ratio of the quantification at different time points, the correlation between low activity and high activity absorbed doses seems on more stable footing. Indeed, the average ratio of 5.3 is consistent with the ratio of administered activities and is consistent with the average value (5.1, determined from the four tumors common to both low activity and high activity 3D analysis) previously determined from a different subset of patients using 3D-RD.³⁴ However, given the wide range of values, it seems that individual patient uptake may vary from administration to administration possibly due to any number of patient or tumor biological factors; therefore, when using pretherapeutic administrations to predict or plan for higher

activity regimens, caution must be taken not to adopt a too literal interpretation of the linear scaling and account for individual discrepancies.

Another interpretation of the results suggests that a hybrid method as described by He et al.,¹¹ for example, where the kinetics of the planar imaging are combined with the absolute quantification of the 3D imaging (SPECT in this case), would likely provide a quantification scheme with a greater accuracy than by planar imaging alone, perhaps comparable with 3D dosimetry. This has generally been admitted (Dewaraja et al.⁴⁴) with the caveat that there are instances where intratumoral uptake and retention vary as a function of time and for which 3D imaging at every time point would still be optimal.⁴⁵ Moreover, the advantage of complete 3D data sets is the ability to run Monte Carlo and score energy within the different volumes of interest (VOIs) from all activity within the field of view. As mentioned, Senthamizchelvan et al.³⁴ have shown for a subset of this same data set that the external dose contribution to tumors can vary up to 10% of the total dose.

As concerns the absolute quantification and the discrepancies observed between the planar and 3D dosimetries, a possible cause for this major difference could be attributed to the particular uptake pattern and large quantities of radiopharmaceutical administered. The background counts used for subtraction tended to be high given that the patients receive up to 400 mCi of activity and that a substantial fraction of this activity was present in the skeleton and that often the regions of uptake included some amount of skeleton to be subtracted.

Recent experience in tumor dosimetry has shown that a single absorbed dose value is unlikely to be predictive of tumor control. Indeed, quantities that take into account tumor heterogeneity such as the equivalent uniform dose are much more likely to correlate with tumor control. This observance has a theoretical basis⁴⁶ and is supported by evidence collected in clinical studies.^{34,47} In addition to the large uncertainties, planar dosimetry is unable to distinguish activity heterogeneity and assumes uniform distribution of activity and a homogeneous composition of the tumor. These conditions will be met in some tumors, but, especially for osteosarcoma, these estimates must be seen as a first-order approximation and more accurate estimates will require an accounting of the density and composition inhomogeneities, as well as the nonuniformity, in absorbed dose. For normal organs, the discrepancies may be less or systematic, in which case planar dosimetry adapted to specific organs such as the posterior view-only approach for kidneys may be adequate.⁴⁸ Additionally, more sophisticated methods of planar quantification have been developed, which are more accurate^{49,50}; however, they are not widely available, nor do they resolve the issue of tumor nonuniform uptake. Indeed, a caveat to the conclusions regarding the levels of uncertainty in planar dosimetry is that this article made use of a particular approach and generalizations regarding the exact accuracy of planar quantification should be made with caution. Direct comparisons with this planar activity quantification would be enlightening; however, the artistic nature of background subtraction in patients and the unequivocal greater uncertainties associated with phantom planar quantification regardless of the methodology urge for a cautious use of planar-based quantification and dosimetry.

From a clinical perspective, experience with external radiotherapy treatment of osteosarcoma suggests that 50–70 Gy are required for this radioresistant tumor.^{51–53} The values presented here are well below this threshold. Higher administered activities will yield higher absorbed doses, increasing the likelihood of therapeutic benefit; however, considering that a similar trial with administered activities of 30.0 mCi/kg has yet to yield significant therapeutic results,¹⁸ the efficacy might be increased by combining targeted radiotherapy for osteogenic sarcoma with other modalities in a combined front-line treatment,⁵⁴ as has been already proven effective for myeloma.²⁷

Conclusions

This study presents retrospective planar tumor dosimetry results as well as an assessment of the uncertainties in tumor activity quantification from WB planar imaging in clinical cases of patients treated with high administered activities of ¹⁵³Sm-EDTMP. Results indicate that absolute planar dosimetry is unreliable and dosimetry using three-dimensional imaging is preferable, particularly for tumors, except perhaps for the most sophisticated planar methods.

Acknowledgments

This article has received support from the National Institutes of Health through the following grants: NIH/NCI 2R01 CA116477 and R01 CA163870.

Disclosure Statement

No competing financial interests exist.

References

1. Flux G, Bardies M, Monsieurs M, et al. The impact of PET and SPECT on dosimetry for targeted radionuclide therapy. *Z Med Phys* 2006;16:47.
2. Jaszczak RJ, Greer KL, Floyd CE, Jr., et al. Improved SPECT quantification using compensation for scattered photons. *J Nucl Med* 1984;25:893.
3. Siegel JA, Wu RK, Maurer AH. The buildup factor: Effect of scatter on absolute volume determination. *J Nucl Med* 1985;26:390.
4. Delpont G, Ferrer L, Lenta C, et al. Comparison of four scatter correction methods for patient whole-body imaging during therapeutic trials with iodine-131. *Cancer* 2002;94(4 suppl):1224.
5. Buvat I, Rodriguez-Villafuente M, Todd-Pokropek A, et al. Comparative assessment of nine scatter correction methods based on spectral analysis using Monte Carlo simulations. *J Nucl Med* 1995;36:1476.
6. Thomas SR, Maxon HR, Kereiakes JG. In vivo quantitation of lesion radioactivity using external counting methods. *Med Phys* 1976;3:253.
7. Bardies M, Bardet S, Faivre-Chauvet A, et al. Bispecific antibody and iodine-131-labeled bivalent hapten dosimetry in patients with medullary thyroid or small-cell lung cancer. *J Nucl Med* 1996;37:1853.
8. Sjogreen K, Ljungberg M, Strand SE. Parameters influencing volume and activity quantitation in SPECT. *Acta Oncol* 1996;35:323.

9. Hobbs RF, Baechler S, Senthamizhchelvan S, et al. A gamma camera count rate saturation correction method for whole-body planar imaging. *Phys Med Biol* 2010;55:817.
10. He B, Du Y, Segars WP, et al. Evaluation of quantitative imaging methods for organ activity and residence time estimation using a population of phantoms having realistic variations in anatomy and uptake. *Med Phys* 2009;36:612.
11. He B, Frey EC. Comparison of conventional, model-based quantitative planar, and quantitative SPECT image processing methods for organ activity estimation using In-111 agents. *Phys Med Biol* 2006;51:3967.
12. Sgouros G, Frey E, Wahl R, et al. Three-dimensional imaging-based radiobiological dosimetry. *Semin Nucl Med* 2008;38:321.
13. Resche I, Chatal JF, Pecking A, et al. A dose-controlled study of ¹⁵³Sm-ethylenediaminetetramethylenephosphonate (EDTMP) in the treatment of patients with painful bone metastases. *Eur J Cancer* 1997;33:1583.
14. Serafini AN, Houston SJ, Resche I, et al. Palliation of pain associated with metastatic bone cancer using samarium-153 lexidronam: A double-blind placebo-controlled clinical trial. *J Clin Oncol* 1998;16:1574.
15. Sartor O, Reid RH, Hoskin PJ, et al. Samarium-153-Lexidronam complex for treatment of painful bone metastases in hormone-refractory prostate cancer. *Urology* 2004;63:940.
16. Sartor O, Reid RH, Bushnell DL, et al. Safety and efficacy of repeat administration of samarium Sm-153 lexidronam to patients with metastatic bone pain. *Cancer* 2007;109:637.
17. Anderson PM, Wiseman GA, Dispenzieri A, et al. High-dose samarium-153 ethylene diamine tetramethylene phosphonate: Low toxicity of skeletal irradiation in patients with osteosarcoma and bone metastases. *J Clin Oncol* 2002;20:189.
18. Anderson PM, Wiseman GA, Erlandson L, et al. Gemcitabine radiosensitization after high-dose samarium for osteoblastic osteosarcoma. *Clin Cancer Res* 2005;11(Pt 1):6895.
19. Loeb DM, Garrett-Mayer E, Hobbs RF, et al. Dose-finding study of (¹⁵³)Sm-EDTMP in patients with poor-prognosis osteosarcoma. *Cancer* 2009;115:2514.
20. Loeb DM, Hobbs RF, Okoli A, et al. Tandem dosing of samarium-153 ethylenediamine tetramethylene phosphoric acid with stem cell support for patients with high-risk osteosarcoma. *Cancer* 2010;116:5470.
21. Loeb DM, Thornton K, Shokek O. Pediatric soft tissue sarcomas. *Surg Clin North Am* 2008;88:615.
22. Essman SC, Lewis MR, Miller WH. Intraorgan biodistribution and dosimetry of ¹⁵³Sm-ethylenediaminetetramethylene phosphonate in juvenile rabbit tibia: Implications for targeted radiotherapy of osteosarcoma. *J Nucl Med* 2005;46:2076.
23. Essman SC, Lewis MR, Fox DB. Effects of increasing doses of samarium-153-ethylenediaminetetramethylene phosphonate on axial and appendicular skeletal growth in juvenile rabbits. *Nucl Med Biol* 2008;35:219.
24. Galiano E, Stradiotto M. A statistical analysis of the initial biodistribution of ¹⁵³Sm-EDTMP in a canine. *Appl Radiat Isot* 2005;63:79.
25. Strigari L, Sciuto R, D'Andrea M, et al. Radiopharmaceutical therapy of bone metastases with ⁸⁹SrCl₂, ¹⁸⁶Re-HEDP and ¹⁵³Sm-EDTMP: A dosimetric study using Monte Carlo simulation. *Eur J Nucl Med Mol Imaging* 2007;34:1031.
26. Brenner W, Kampen WU, Kampen AM, et al. Skeletal uptake and soft-tissue retention of ¹⁸⁶Re-HEDP and ¹⁵³Sm-EDTMP in patients with metastatic bone disease. *J Nucl Med* 2001;42:230.
27. Kendler D, Donnemiller E, Oberladstatter M, et al. An individual dosimetric approach to ¹⁵³Sm-EDTMP therapy for pain palliation in bone metastases in correlation with clinical results. *Nucl Med Commun* 2004;25:367.
28. Dispenzieri A, Wiseman GA, Lacy MQ, et al. A phase I study of ¹⁵³Sm-EDTMP with fixed high-dose melphalan as a peripheral blood stem cell conditioning regimen in patients with multiple myeloma. *Leukemia* 2005;19:118.
29. Eary JF, Collins C, Stabin M, et al. Samarium-153-EDTMP biodistribution and dosimetry estimation. *J Nucl Med* 1993;34:1031.
30. Fizazi K, Beuzebec P, Lumbroso J, et al. Phase II trial of consolidation docetaxel and samarium-153 in patients with bone metastases from castration-resistant prostate cancer. *J Clin Oncol* 2009;27:2429.
31. Morris MJ, Pandit-Taskar N, Carrasquillo J, et al. Phase I study of samarium-153 lexidronam with docetaxel in castration-resistant metastatic prostate cancer. *J Clin Oncol* 2009;27:2436.
32. Bayouth JE, Macey DJ. Dosimetry considerations of bone-seeking radionuclides for marrow ablation. *Med Phys* 1993;20:1089.
33. Bayouth JE, Macey DJ, Kasi LP, et al. Dosimetry and toxicity of samarium-153-EDTMP administered for bone pain due to skeletal metastases. *J Nucl Med* 1994;35:63.
34. Senthamizhchelvan S, Hobbs RF, Song H, et al. Tumor dosimetry and response for ¹⁵³Sm-ethylenediamine tetramethylene phosphonic acid therapy of high-risk osteosarcoma. *J Nucl Med* 2012;53:215.
35. Hobbs RF, Prideaux AR, Baechler S, et al. Tumor dosimetry of patients treated for osteosarcoma with ¹⁵³Sm-EDTMP. European Association of Nuclear Medicine Annual Meeting Abstracts Oct 2008.
36. He B, Wahl RL, Du Y, et al. Comparison of residence time estimation methods for radioimmunotherapy dosimetry and treatment planning—Monte Carlo simulation studies. *IEEE Trans Med Imaging* 2008;27:521.
37. Siegel JA, Thomas SR, Stubbs JB, et al. MIRD pamphlet no. 16: Techniques for quantitative radiopharmaceutical biodistribution data acquisition and analysis for use in human radiation dose estimates. *J Nucl Med* 1999;40:37S.
38. Prideaux AR, Song H, Hobbs RF, et al. Three-dimensional radiobiologic dosimetry: Application of radiobiologic modeling to patient-specific 3-dimensional imaging-based internal dosimetry. *J Nucl Med* 2007;48:1008.
39. Hobbs RF, Wahl RL, Lodge MA, et al. ¹²⁴I PET-based 3D-RD dosimetry for a pediatric thyroid cancer patient: Real-time treatment planning and methodologic comparison. *J Nucl Med* 2009;50:1844.
40. Stabin MG, Sparks RB, Crowe E. OLINDA/EXM: The second-generation personal computer software for internal dose assessment in nuclear medicine. *J Nucl Med* 2005;46:1023.
41. Wambersie A, DeLuca P. ICRU Report 67: Absorbed-Dose Specification in Nuclear Medicine. Ashford, Kent, GB, 2002.
42. Williams LE, Duda RB, Proffitt RT, et al. Tumor uptake as a function of tumor mass: A mathematic model. *J Nucl Med* 1988;29:103.

43. Boswell CA, Brechbiel MW. Development of radioimmunotherapeutic and diagnostic antibodies: An inside-out view. *Nucl Med Biol* 2007;34:757.
44. Dewaraja YK, Frey EC, Sgouros G, et al. MIRD pamphlet No. 23: Quantitative SPECT for patient-specific 3-dimensional dosimetry in internal radionuclide therapy. *J Nucl Med* 2012; 53:1310.
45. Sgouros G, Kolbert KS, Sheikh A, et al. Patient-specific dosimetry for ^{131}I thyroid cancer therapy using ^{124}I PET and 3-dimensional-internal dosimetry (3D-ID) software. *J Nucl Med* 2004;45:1366.
46. Niemierko A. Reporting and analyzing dose distributions: A concept of equivalent uniform dose. *Med Phys* 1997;24:103.
47. Dewaraja YK, Schipper MJ, Roberson PL, et al. 131I-tositumomab radioimmunotherapy: Initial tumor dose-response results using 3-dimensional dosimetry including radiobiologic modeling. *J Nucl Med* 2010;51:1155.
48. Baechler S, Hobbs RF, Prideaux AR, et al. Estimates of radiation-absorbed dose to kidneys in patients treated with 90Y-ibritumomab tiuxetan. *Cancer Biother Radiopharm* 2008;23:633.
49. Song N, He B, Wahl RL, et al. EQPlanar: A maximum-likelihood method for accurate organ activity estimation from whole-body planar projections. *Phys Med Biol* 2011; 56:5503.
50. He B, Wahl RL, Sgouros G, et al. Comparison of organ residence time estimation methods for radioimmunotherapy dosimetry and treatment planning—patient studies. *Med Phys* 2009;36:1595.
51. Hristov B, Shokek O, Frassica DA. The role of radiation treatment in the contemporary management of bone tumors. *J Natl Compr Canc Netw* 2007;5:456.
52. Kaushal A, Citrin D. The role of radiation therapy in the management of sarcomas. *Surg Clin North Am* 2008;88: 629.
53. Welsh JS, Thurman SA, Borzillary S, et al. Sm-153 EDTMP for recurrent metastatic osteosarcoma. *Clin Adv Hematol Oncol* 2003;1:181; discussion 183.
54. Hobbs RF, McNutt T, Baechler S, et al. A treatment planning method for sequentially combining radiopharmaceutical therapy and external radiation therapy. *Int J Radiat Oncol Biol Phys* 2011;80:1256.